Open access • Journal Article • DOI:10.1063/1.468875

The F+HD --> DF(HF)+H(D) reaction revisited: Quasiclassical trajectory study on an ab initio potential energy surface and comparison with molecular beam experiments

F. J. Aoiz, Luis Bañares, Víctor J. Herrero, V. Sáez Rábanos ...+2 more authors

Published on: 15 Jun 1995 - Journal of Chemical Physics (American Institute of Physics)

Topics: Potential energy surface and Ab initio

The F+HD→DF(HF)+H(D) reaction revisited: Quasiclassical trajectory study on an ab initio potential energy surface and comparison with molecular beam experiments

F. J. Aoiz, L. Bañares, V. J. Herrero, V. Sáez Rábanos, K. Stark et al.

Citation: J. Chem. Phys. **102**, 9248 (1995); doi: 10.1063/1.468875
View online: http://dx.doi.org/10.1063/1.468875
View Table of Contents: http://jcp.aip.org/resource/1/JCPSA6/v102/i23
Published by the American Institute of Physics.

The F+HD→DF(HF)+H(D) reaction revisited: Quasiclassical trajectory study on an *ab initio* potential energy surface and comparison with molecular beam experiments

F. J. Aoiz and L. Bañares
Departamento de Química Física, Facultad de Química, Universidad Complutense, 28040 Madrid, Spain

V. J. Herrero
Instituto de Estructura de la Materia (CSIC), Serrano 123, 28006 Madrid, Spain

V. Sáez Rábanos
Departamento de Química General y Bioquímica, ETS Ingenieros de Montes, Universidad Politécnica, 28040 Madrid, Spain

K. Stark and H.-J. Werner
Institut für Theoretische Chemie, Universität Stuttgart, Pfaffenwaldring 55, D-70569 Stuttgart, Germany

(Received 3 January 1995; accepted 15 March 1995)

The dynamics of the F+HD reaction has been studied by means of quasiclassical trajectory calculations on an *ab initio* potential energy surface (PES) at several collision energies. At the collision energy of 85.9 meV and for the DF+H isotopic channel of the reaction, there is a remarkable agreement between calculated and experimental results, in both the center of mass (c.m.) differential cross sections (DCS) and in the simulation of the laboratory (LAB) time of flight (TOF) and angular distributions (AD). The good agreement also extends to the lower collision energy of 58.6 meV for this channel of the reaction. In contrast, the simulation of the LAB angular distributions for the HF+D channel shows strong discrepancies between theory and experiment at both collision energies, which can be traced back to the absence of a forward peak in the calculated c.m. DCS for HF($v'=3$). Simulations made from QCT calculations on other PES with important HF($v'=3$) forward scattering contributions also fail to reproduce the overall AD. The theoretical findings and especially the roles of translational energy and initial rotational momentum on the dynamics of this reaction are discussed in terms of the topology of the PES through the analysis of individual trajectories. © *1995 American Institute of Physics.*

I. INTRODUCTION

In recent times, decisive progresses, both experimental and theoretical, have been made towards a precise knowledge of the $F+H_2 \rightarrow HF+H$ reactive system. This reaction has been for decades a prototype in the field of molecular dynamics and has played a key role in most studies about the influence of quantum mechanical resonances in reactive scattering. Exact quantum mechanical (QM), quasiclassical trajectory (QCT) and semiclassical calculations of the collinear reaction probability for the $F+H_2 \rightarrow HF+H$ and its isotopic analogs, resolved into the products' vibrational states, were performed by Schatz, Bowman and Kuppermann[1–3] on the Muckerman 5 (M5)[4] potential energy surface (PES) in the early seventies. These calculations revealed the presence of large quantum effects that were associated with scattering resonances.[1–7] The mentioned resonance effects were manifest as maxima in the collinear reaction probability as a function of collision energy (E_T) for the processes leading from ground state molecular reactants to HF($v'=2$) and DF ($v'=3$). Other collinear QM calculations showed that the resonance structure was strongly dependent on the PES.[8] The possible survival of resonance effects in accurate three dimensional (3D) quantum mechanical calculations remained an open question at the time, but approximate 3D QM calculations on the M5 PES[9–11] did not lead to sharp structures in the energy evolution of the reaction probability or cross section.

Experimentally, the $F+H_2$ reaction was intensively studied during the sixties and seventies by several techniques.[12–15] Of particular interest for the detailed dynamical calculations commented on above, were the molecular beam experiments performed by the group of Lee.[14,15] One of these experiments[15] showed that the center of mass (c.m.) differential cross section (DCS) for the production of HF($v'=2$) changed from backward peaked (the backward direction being the opposite to that of the incoming atom), at a collision energy of $E_T=0.09$ eV, to slightly sideways peaked at $E_T=0.14$ eV. With the experimental data then available, the scattering into the rest of the HF vibrational levels remained essentially backward. A tendency of the DCS for HF($v'=2$) towards sideways or forward peaking with increasing E_T was obtained in approximate 3D quantum mechanical calculations performed on the M5 PES.[10,16–20] A possible resonance in reactive scattering should lead to a broadening of the DCS due to the formation of a short-lived complex and this was the interpretation favored,[10,16–19] although it was not unanimously established[20] in the theoretical analysis of the HF($v'=2$) sidewards scattering at $E_T \approx 0.14$ eV.

A major breakthrough in the study of the prototypic $F+H_2$ reactive system was achieved in the famous high reso-

 0021-9606/95/102(23)/9248/15/$6.00

lution molecular beam experiments reported by Lee and coworkers in 1985.[21,22] The most interesting dynamical feature disclosed by these measurements was the appearance of forward peaks in the c.m. DCS for the scattering of HF ($v'=3$) from the $F+H_2$ reactive encounters in the collision energy range between 0.08 and 0.15 eV. A smaller forward peak was also observed for the scattering of DF($v'=4$) from $F+D_2$ at $E_T=0.144$ eV. For the rest of the vibrational states of HF and DF, the scattering was predominantly in the backward direction. In spite of the fact that at the time of the measurements no theoretical calculation neither classical[23–25] nor quantum mechanical[10,16,18–20,23] on any of the existing surfaces and, most notably, on the widely used and strongly collinear M5 PES, could reproduce the state selective forward peaks observed in the experiments, these newly discovered features were again regarded as the most promising evidence of a quantum mechanical resonance in reactive scattering, unlikely to be explained by classical mechanics considerations.[21,22] The discrepancies between experiment and theory were attributed to failures of the PES.

The construction of new empirical[26] and semiempirical PES[27–30] allowed the qualitative reproduction of the DCS forward peaks in dynamical calculations, both quantum mechanical[30–32] and classical.[26,33–36] After these works, it became generally accepted that the relevant PES for this reaction has a bent transition state and a comparatively flat angular barrier to reaction. Nevertheless, the mentioned dynamical calculations on the new surfaces led to disagreements with other well established experimental results, such as product states distributions,[12,13,21,22] reaction rate constants[37–39] or photoelectron spectra.[40–43] Moreover, the fact that the DCS state selective forward peaks also appear in the quasiclassical trajectory results cast serious doubts on their interpretation as a manifestation of QM scattering resonances.

Recently, a new and totally *ab initio* PES for this reaction has been constructed by Stark and Werner (SW).[44–46] Accurate QM calculations performed using this surface could account for the electron photodetachment spectra of the FH_2^- ion obtained by Neumark and co-workers.[47] These experiments sample basically the transition state region of the potential energy surface. The asymptotic properties of reactive scattering on this PES have also been investigated. QCT calculations on the SW PES[45,48] have revealed substantial accordance with the experimentally deduced CM differential cross sections and with the product state distributions reported by Lee and coworkers for $F+H_2$ and $F+D_2$ reactions,[21,22] as well as with the recent and higher resolution data of Faubel *et al.* about $F+D_2$.[49] In particular, the tendency from backwards to sideways peaking of HF($v'=2$) scattering with increasing E_T and the state selective forward peaks in the DCS of HF($v'=3$) and DF($v'=4$), which had been succesively attributed to QM resonances, are obtained in these classical calculations. Although some discrepancies still persist, the results of the mentioned QCT calculations on the SW PES provide the best global description to date of the experimental findings about the dynamics of this reaction.

A noteworthy difference between the experimentally deduced DCS for $F+H_2$ and those from QCT on the SW surface lies in the size of the forward peaks, the theoretical ones being smaller.[45] Accurate QM calculations presently performed by Manolopoulos *et al.*[50] show that the forward peaks are substantially increased in the quantum calculations. This is also indicated by the comparison of QCT and exact QM differential cross sections for $F+H_2(j=0,1)$ on the semiempirical 6SEC PES.[30,35] In this case, the classical forward peak was much enhanced in the quantal calculation. The accordance between the QCT calculations on the SW PES and the experimental data is, however, better for the $F+D_2$ isotopic variant of the reaction.[48] In this case, the forward peaks deduced from the experiment are satisfactorily reproduced and it is possible to simulate the recent high resolution time of flight (TOF) spectra[49] directly with the theoretical results.

In view of this situation, a theoretical investigation of the F+HD reaction, for which cross-beam measurements are also available, seems now timely. From a dynamical point of view, this isotopic variant is the richest one since the attack of the fluorine atom to the two distinct ends of the molecule samples different regions of the PES and provides thus a more stringent test for a theoretical approach than the symmetric $F+H_2$ and $F+D_2$ reactions. Taking that into account, we have performed extensive QCT calculations of the dynamics of the F+HD reaction on the SW PES for the range of experimental conditions of the molecular beam experiments of Neumark *et al.* The calculations include state resolved integral and differential cross sections and reaction probabilities as a function of impact parameter for the two isotopic output channels. In order to compare more precisely with the measurements, we have undertaken the full simulation of the primary experimental data, i.e., angular distributions and time of flight spectra in the laboratory frame. The QCT results are analyzed in terms of the characteristics of the potential energy surface.

II. METHOD

The general method of calculation of quasiclassical trajectories is the same one as used in previous works. It is described more extensively in Refs. 51 and 52 and only the particular details relevant to the present work will be given here.

The calculations on the *ab initio* SW potential energy surface have been performed for the F+HD ($v=0$, $j=0,1$) reaction at collision energies of 58.6 meV (1.35 kcal mol^{-1}) and 85.9 meV (1.98 kcal mol^{-1}), corresponding to average collision energies of the molecular beam experiments of Neumark *et al.*,[22] and at the collision energy of 148 meV (3.42 kcal mol^{-1}). Batches of about 50 000 to 60 000 trajectories have been calculated at each energy and initial rotational quantum number j. In addition, batches of 24 000 and 60 000 trajectories have been calculated for the title reaction at 85.9 meV and initial $j=0$ on the 6SEC PES of Truhlar and co-workers[30] and on the empirical Takayanagi and Sato (T-S) PES,[26] respectively, to compare with the results on the SW PES.

The initial rovibrational energies of the HD molecule are calculated using a Dunhan expansion containing 16 terms[53–55] [fifth power in $v+(1/2)$ and third power in $j(j$

$+1)]$. For the assignment of product quantum numbers, the classical HF (DF) molecule rotational angular momentum is equated to $[j'(j'+1)]^{1/2}\hbar$. With the (real) j' value so obtained, the vibrational quantum number v' is found by equating the internal energy of the outgoing molecule to the corresponding rovibrational Dunham expansion.[53] The values of v' and j' found in this way are then rounded to the nearest integer.

The vibrationally state resolved differential cross sections, $d^2\sigma/d\omega$, were calculated by the method of moments expansion in Legendre polynomials (see Refs. 52, 56, and 57). The Smirnov–Kolmogorov test comparing the cumulative probability distributions was used to decide when to truncate the series. Significance levels higher than 95% could be achieved using 8–12 Legendre moments, ensuring a very good convergence such that the inclusion of more terms does not produce any significant change. Special care was paid to the analysis of particular structures in the differential cross sections which remain unaffected when the number of Legendre moments are changed in ± 2. The error bars, calculated as in Ref. 52, correspond to plus/minus one standard deviation. The reaction probabilities as a function of the impact parameter (opacity functions) were also calculated using the method of moments expansion in Legendre polynomials as described in Ref. 52. The assumed correspondence between the orbital angular momentum quantum number, l, and the impact parameter, b, is $l(l+1)\hbar^2=2\mu E_T b^2$, where μ is the reagents reduced mass and E_T the collision energy.

Angle-velocity contour polar maps are derived from the full v',j' state resolved differential cross sections, $d^2\sigma(v',j')/d\omega$. Since the measurements could not resolve the rotational structure, to make the calculated c.m. polar maps directly comparable with the experiment, some broadening effect needs to be included, and, similarly to Refs. 45, 48, 58, and 59, this is done by assuming a spread in the products' center of mass (c.m.) recoil velocity of Gaussian shape. The final expression for the c.m. angle-velocity distribution is given by

$$P(w,\theta)=\sum_{k=1}^{n}\left(\frac{d^2\sigma}{d\omega}\right)_k N_k \exp\left[-\left(\frac{w-w_k}{\Delta w_k}\right)^2\right], \tag{1}$$

where the sum extends to all the final v',j' states which are energetically accessible. The experimental uncertainty in w is modelled with a Gaussian distribution centered in every case at w_k, the recoil velocity associated with the internal state k, and with a width Δw_k. The N_k are the normalization constants of the Gaussian profiles. The FWHM, given by $2(\ln 2)^{1/2}\Delta w_k/w_k$, was 10% in all the cases, which corresponds to 20% of uncertainty in the c.m. energy of the DF product.

The simulation of the laboratory (LAB) time-of-flight (TOF) spectra of scattered DF and HF molecules is carried out by transforming the theoretical c.m. v',j' DCS into the LAB system.[60] The signal at a given time t and LAB angle Θ can be cast as:

$$\begin{aligned} I(t;\Theta)=&\sum_j P(j)\int d^3\mathbf{r}\int\int dv_1 dv_2 f(v_1)\\ &\times f(v_2) n_1(\mathbf{r}) n_2(\mathbf{r}) v_r\\ &\times\sum_p\left(\frac{d^2\sigma}{d\omega}\right)_p\sum_{q=1,2}\frac{v_{pq}^2}{w_p^2|\cos\,\xi_{pq}|}\frac{t_{pq}}{L}\\ &\times H[t_{pq}-(t_0-\delta)]H[(t_0+\delta)-t_{pq}]. \end{aligned} \tag{2}$$

The procedure, similar to those of Refs. 61 and 62, consists on a Monte Carlo sampling of the reagents' beam velocities, v_1 and v_2, with distributions $f(v_1)$ and $f(v_2)$, and spatial beam densities $n_1(\mathbf{r})$ and $n_2(\mathbf{r})$, where the position vector $\mathbf{r}$ refers to a point into the scattering volume defined by the beam divergences and the geometry of the experiment.[21,22] In this equation, v_r is the relative velocity, v_{pq} and w_p are the LAB and c.m. velocities of the HF (DF) product, respectively, and ξ_{pq} is the angle between v_{pq} and w_p. The sum in p extends to all the final vibrorotational v',j' states energetically accessible. The sum running in $q=1,2$ takes into account that for a given quantum state of the products there might be, at a given Θ, fast and slow products in the LAB system (which will be labeled as $+$ and $-$, respectively). The factor $t_{pq}/L=1/v_{pq}$ accounts for the number density detection,[60] where t_{pq} is the time of flight of the products formed in the p state before ionization and L the flight length. The Heaviside step functions, $H(x)$ (equal to 1 if $x>0$ and equal to 0 if $x<0$), are used to indicate that only those times t_{pq} within the interval $(t_0-\delta,t_0+\delta)$, where $2\delta=8\,\mu$s/channel (the counting time resolution)[21] are included. The final time t is the sum of t_0, the neutral HF (DF) time of flight, t_i, the ion time of flight inside the mass spectrometer, and $t_{\mathrm{HD}}(\mathbf{r},v_2)$ the time needed by the HD molecules to reach the scattering volume from the random chopper. The experimental parameters for the simulation were directly taken from Refs. 21 and 22 and a flight length L of 33 cm was used.[63]

The LAB angular distributions (AD) are simulated in a similar way by integrating in either the velocity or time space. In the former case, the signal at an angle Θ can be expressed as

$$\begin{aligned} S(\Theta)=&\sum_j P(j)\int d^3\mathbf{r}\int\int dv_1\,dv_2\\ &\times f(v_1) f(v_2) n_1(\mathbf{r}) n_2(\mathbf{r}) v_r\\ &\times\sum_p\left(\frac{d^2\sigma}{d\omega}\right)_p\sum_{q=1,2}\frac{v_{pq}}{w_p^2|\cos\,\xi_{pq}|}, \end{aligned} \tag{3}$$

where all the variables are as in Eq. (2).

In the two cases [Eqs. (2) and (3)], the angular resolution of the detector (1.25°) is also taken into account. All the simulations of the LAB and c.m. experimental results for the F+HD reaction[22] are made by appropriately weighting on the initial rotational quantum number j of the HD reagent, indicated in Eqs. (2) and (3) as the sum on j, where $P(j)$ are the corresponding weights taken as 0.90 and 0.10 for $j=0$ and $j=1$, respectively, according to Ref. 22.

TABLE I. Comparison of QCT integral cross sections $\sigma_R(\text{Å}^2)$ for the production of DF(v') at the collision energies of 58.6, 85.9 and 148 meV. Values in parentheses are the branching ratios defined as $\sigma_R(v')/\sigma_R(v'=3)$.

E_T=58.6 meV Surface	$v'=1$	$v'=2$	$v'=3$	$v'=4$	all v'
SW ($j=0$)	⋯	0.12 (0.32)	0.38 (1.0)	0.42 (1.11)	0.92
SW ($j=1$)	0.003(0.006)	0.29 (0.56)	0.52 (1.0)	0.36 (0.69)	1.17
E_T=85.9 meV Surface	$v'=1$	$v'=2$	$v'=3$	$v'=4$	all v'
6SEC ($j=0$)	⋯	0.21 (0.34)	0.63 (1.0)	0.75 (1.19)	1.59
T-S ($j=0$)	⋯	0.64 (0.40)	1.59 (1.0)	1.25 (0.79)	3.48
SW ($j=0$)	0.004 (0.004)	0.53 (0.52)	1.02 (1.0)	0.81 (0.79)	2.36
SW ($j=1$)	0.034 (0.003)	0.64 (0.59)	1.08 (1.0)	0.71 (0.66)	2.46
SW (thermal)	0.007 (0.007)	0.54 (0.52)	1.03 (1.0)	0.80 (0.78)	2.38
Experiment	(0.02)	(0.40)	(1.0)	(0.48)	
E_T=148 meV Surface	$v'=1$	$v'=2$	$v'=3$	$v'=4$	all v'
SW ($j=0$)	0.45 (0.24)	1.58 (0.83)	1.91 (1.0)	0.53 (0.28)	4.47
SW ($j=1$)	0.22 (0.14)	1.18 (0.78)	1.52 (1.0)	0.71 (0.47)	3.63

III. RESULTS

Tables I and II summarize the calculated vibrationally resolved and total integral cross sections on the SW PES for the two isotopic channels of the reaction, DF+H and HF+D, respectively, at three collision energies and initial rotational quantum numbers $j=0$ and $j=1$. For comparison purposes, the $\sigma_R(v')$ obtained at 85.9 meV of collision energy and initial rotational quantum number $j=0$ on the T-S[26] and 6SEC PES,[30] that have been calculated in this work, are also presented. None of these values are corrected for the fact that there are two competing potential surfaces that correlate with the ground state reagents (although only one of these states correlates with the products' electronic ground state). The present calculations, purely adiabatic, ignore absolutely the existence of this upper PES and no multisurface factor is included (see Ref. 48 and references therein).

The comparison with the results obtained on other PES at initial $j=0$ and E_T=85.9 meV shows that, overall, the absolute values of the total integral cross sections calculated on the SW PES are in between those obtained previously for this reaction on the T-S, M5, 5SEC[34] and 6SEC PES.

From Tables I and II it can be seen that, at the collision energies and initial j studied in this work, the DF yield is always greater than the one for HF in the calculations on the SW PES. The isotopic branching ratio, defined as $\Gamma=\sigma_R(\text{DF})/\sigma_R(\text{HF})$, increases rapidly with collision energy in the range here studied for intitial $j=0$, whereas for $j=1$ it does more slowly. In general terms, it seems that collision

TABLE II. Comparison of QCT integral cross sections $\sigma_R(\text{Å}^2)$ for the production of HF(v') at the collision energies of 58.6, 85.9 and 148 meV. Values in parentheses are the branching ratios defined as $\sigma_R(v')/\sigma_R(v'=2)$.

E_T=58.6 meV Surface	$v'=0$	$v'=1$	$v'=2$	$v'=3$	all v'
SW ($j=0$)	⋯	⋯	0.31 (1.0)	0.21 (0.68)	0.52
SW ($j=1$)	⋯	0.074 (0.10)	0.75 (1.0)	0.35 (0.47)	1.17
E_T=85.9 meV Surface	$v'=0$	$v'=1$	$v'=2$	$v'=3$	all v'
6SEC ($j=0$)	⋯	0.11 (0.10)	1.08 (1.0)	0.79 (0.73)	1.98
T-S ($j=0$)	⋯	0.15 (0.17)	0.86 (1.0)	0.56 (0.65)	1.57
SW ($j=0$)	⋯	0.15 (0.22)	0.69 (1.0)	0.24 (0.35)	1.08
SW ($j=1$)	⋯	0.38 (0.30)	1.25 (1.0)	0.44 (0.35)	2.07
E_T=148 meV Surface	$v'=0$	$v'=1$	$v'=2$	$v'=3$	all v'
SW ($j=0$)	0.01 (0.02)	0.30 (0.59)	0.51 (1.0)	0.16 (0.31)	0.98
SW ($j=1$)	0.13 (0.10)	0.85 (0.63)	1.36 (1.0)	0.42 (0.31)	2.76

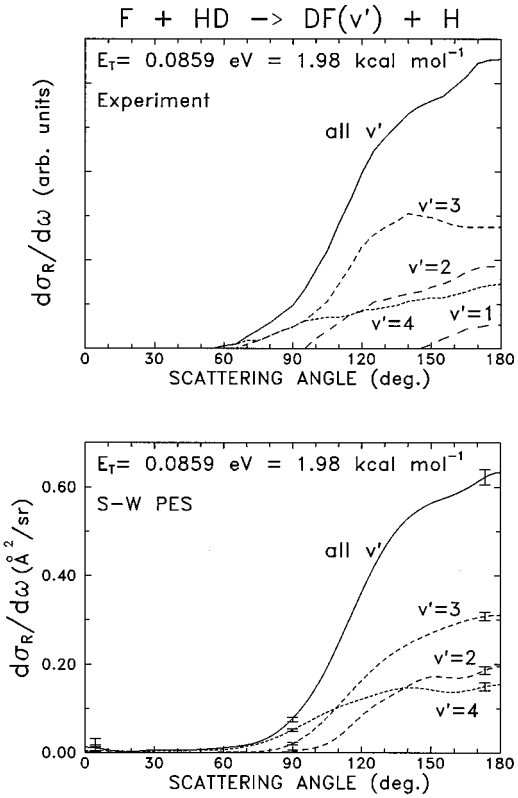

FIG. 1. Comparison of the experimentally deduced (Ref. 22) c.m. solid angle differential cross sections resolved into the final vibrational states of the products for the F+HD→DF+H reaction (upper panel) and the calculated with QCT on the SW PES (lower panel). The latter are weighted on the initial rotational quantum number j (90% in $j=0$ and 10% in $j=1$) according to the experimental HD molecule rotational temperature (Ref. 22).

energy tends to favor DF formation, whereas rotation of HD promotes the HF channel. At $E_T=85.9$ meV and $j=0$, Γ is 2.2 on the SW PES, exactly the same as on the T-S PES and quite close to its value on the M5 PES.[34] However, in contrast with the other PES, on the 6SEC PES $\Gamma=0.80$ (0.88 on the 5SEC[34]), thus favoring the production of HF molecules.

The role of the collision energy and initial rotational quantum number j in the total integral cross section for this reaction on the SW PES is noteworthy. The total cross section for the production of DF molecules increases rapidly with collision energy for initial $j=0$. In contrast, HD rotation is not efficient in promoting reaction into this channel and, at the highest collision energy presented in Table I, the absolute cross section even decreases in going from $j=0$ to $j=1$. The branching ratios into the different product vibrational states, defined as $\sigma_R(v')/\sigma_R(v'=3)$ (shown in parentheses in Table I), also change significantly with collision energy. At low collision energy, $v'=4$ seems to be the most favored DF vibrational state, whereas at the highest collision energy the absolute cross section into this channel decreases in such a way that its branching ratio becomes smaller than those for the production of DF molecules in $v'=3$ and $v'=2$. The opposite tendency is followed by DF in $v'=1$ and $v'=2$. The addition of one quantum in HD rotation seems to mitigate this effect. At the intermediate collision energy and $j=0$, the cross sections into the DF channel calculated on the T-S PES are always larger than the ones given by the SW PES, although the branching ratios are quite similar. On the other hand, the cross sections calculated on the 6SEC PES are substantially smaller and the branching ratios indicate a higher vibrational excitation of the DF product.

The experimental branching ratios,[22] only available for the F+HD→DF+H reaction at $E_T=85.9$ meV, are also presented in Table I. The main discrepancy lies in the yield into $v'=4$ which is overestimated in the QCT calculations on the SW PES as compared with the experimental results. This discrepancy extends to the calculations carried out on other PES (T-S, 5SEC and 6SEC) with the exception of the M5 PES, where the agreement is noticeable (see Table I and Ref. 34).

The role of translation and rotation is reversed in the HF isotopic channel of the reaction as shown in Table II. Whereas translational energy is quite unefficient in promoting the reaction leading to HF in the range of collision energies considered, the cross sections at all the energies increase considerably when going from $j=0$ to $j=1$. As in the case of the DF isotopic channel, rotation and, to a lesser extent, collision energy favor the formation of the HF product in low

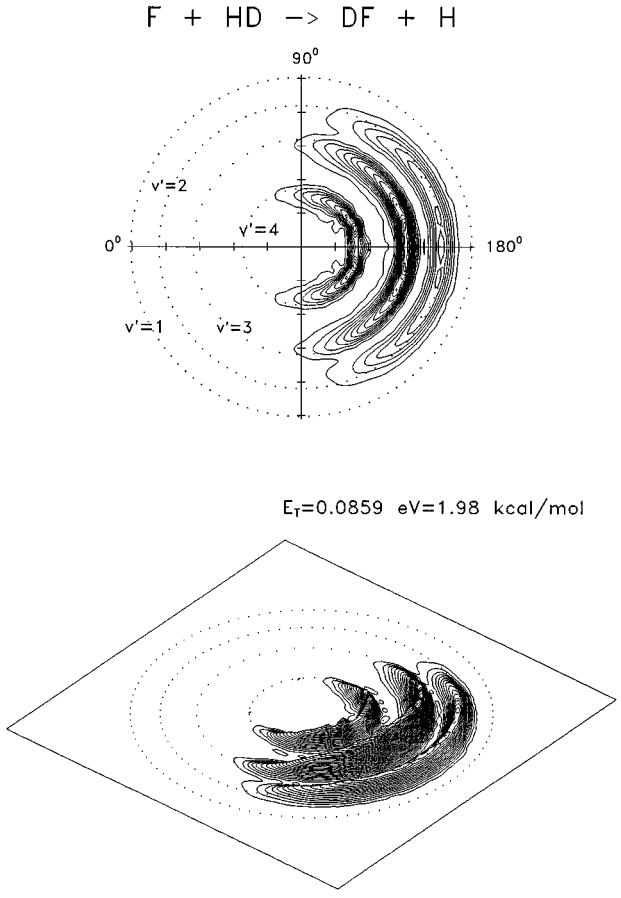

FIG. 2. Calculated angle-velocity contour polar map and its 3D perspective of the F+HD→DF+H reation channel on the SW PES at the indicated collision energy, corresponding to the mean value of the experiment of Ref. 22 and weighted on initial j as in Fig. 1. The dotted circles represent the maximum DF recoil velocity at each vibrational state. The separation between the ticks of the axes is 200 m s^{-1}.

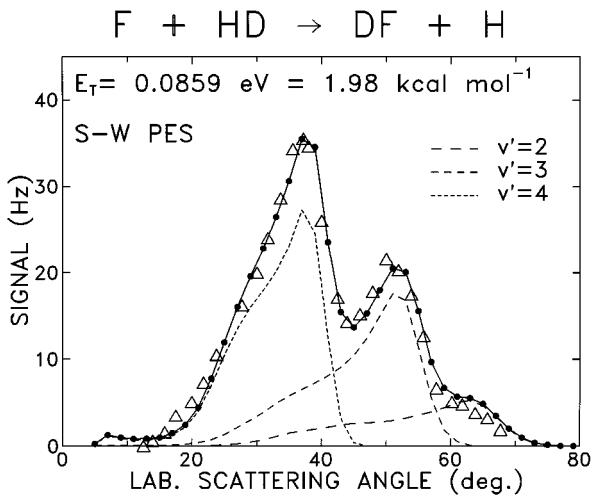

FIG. 3. Experimental (triangles) and simulated (solid circles and solid line through the points) laboratory (LAB) angular distribution for the DF+H channel of the title reaction at the indicated collision energy. The different dashed lines correspond to the calculated vibrationally state resolved LAB angular distributions as indicated in the figure. The simulation is done by using the QCT calculated differential cross sections on the SW PES and the adequate c.m. to LAB transformation taking into account the characteristics of the molecular beam experiments (see Sec. II).

v' states. The cross sections from the 6SEC PES, at E_T=85.9 meV, are considerably larger than those obtained on the SW PES, while the ones from the T-S PES are in between. Both in the T-S and 6SEC surfaces, the branching ratios, defined for this channel as $\sigma_R(v')/\sigma_R(v'=2)$ (see Table II), are smaller for $v'=1$ and larger for $v'=3$ than those calculated on the SW PES.

The only c.m. differential cross section experimentally available for this reaction reported in Ref. 22 is for the DF channel at 85.9 meV (1.98 kcal/mol) of collision energy. Product's time-of-flight spectra at several LAB scattering angles, as well as the LAB angular distribution, were recorded for this isotopic channel at the mentioned energy. By fitting these primary data, including the proper convolution with the experimental broadening effects, the vibrationally resolved c.m. DCS and angle-velocity polar maps could be deduced.[22] The QCT vibrationally resolved DCS for the F+HD→DF(v')+H reaction at E_T=85.9 meV calculated on the SW PES for the conditions of the experiments of Neumark *et al.*[22] (90% of HD in $j=0$ and the remaining 10% in $j=1$) are compared in Fig. 1 to the experimentally deduced DCS. The overall agreement between experiment and theory is indeed very good for each of the DF vibrational states. The worst agreement is obtained for the DF($v'=3$) and is mainly due to the greater sideways character of the experimental $v'=3$ resolved DCS as compared with the QCT one. In addition, the QCT $v'=4$ resolved DCS is larger than the experimental one in the c.m. scattering angle range between 90° and 150°. These discrepancies between theory and experiment explain the differences observed in the experimental and calcultated branching ratios into final vibrational states as commented on above. The influence of the

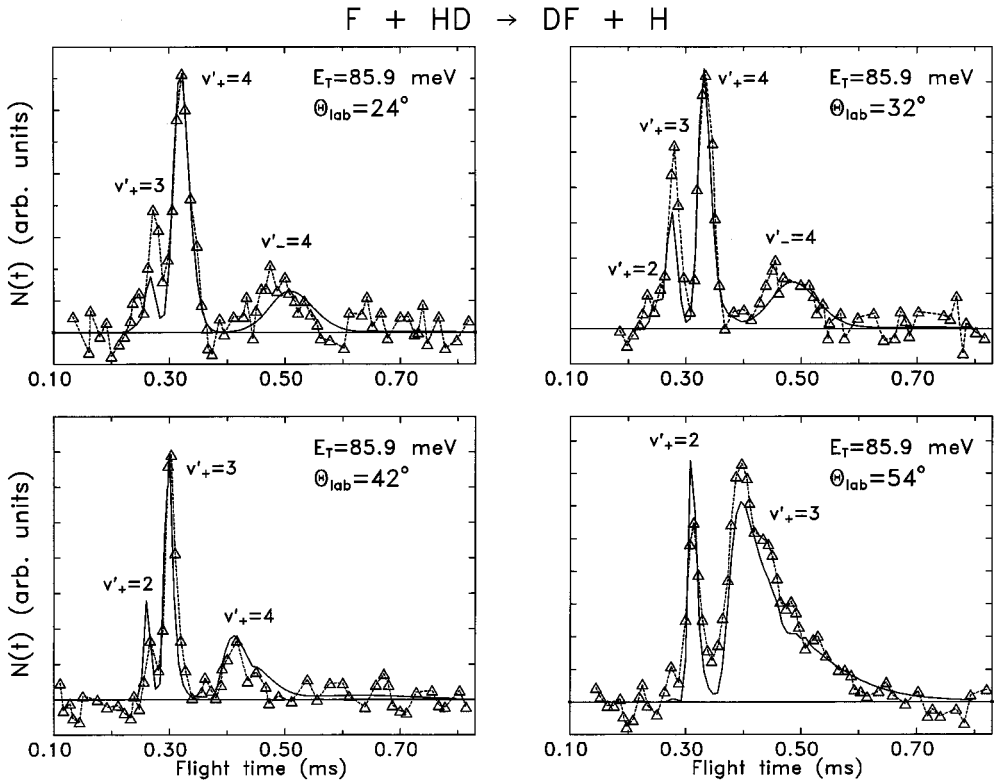

FIG. 4. Experimental (Ref. 22) (triangles and dashed lines) vs simulated (solid lines) time-of-flight spectra at the indicated LAB angles. The peaks are labeled with the corresponding vibrational states of the DF product. The +/− subindices are used to distinguish between scattering to the right/left of the relative velocity, leading to fast/slow DF molecules in the LAB frame.

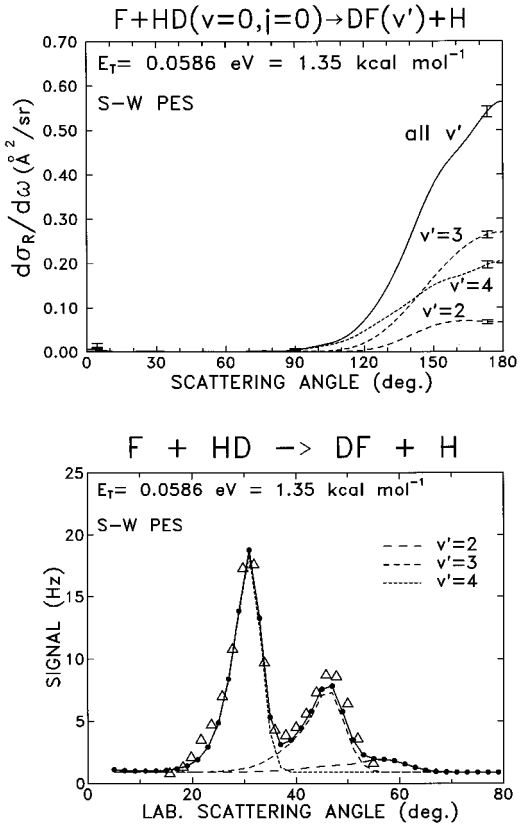

FIG. 5. Top: QCT c.m. differential cross sections for the F+HD $(v=0,j=0)\rightarrow$DF+H reaction at $E_T=58.6$ meV calculated on the SW PES, resolved into the final v' states of DF. Bottom: LAB angular distribution at this collision energy. The triangles correspond to the experimental data from Ref. 22 and the solid circles and solid line to the theoretical simulation. The different dashed lines are as in Fig. 3.

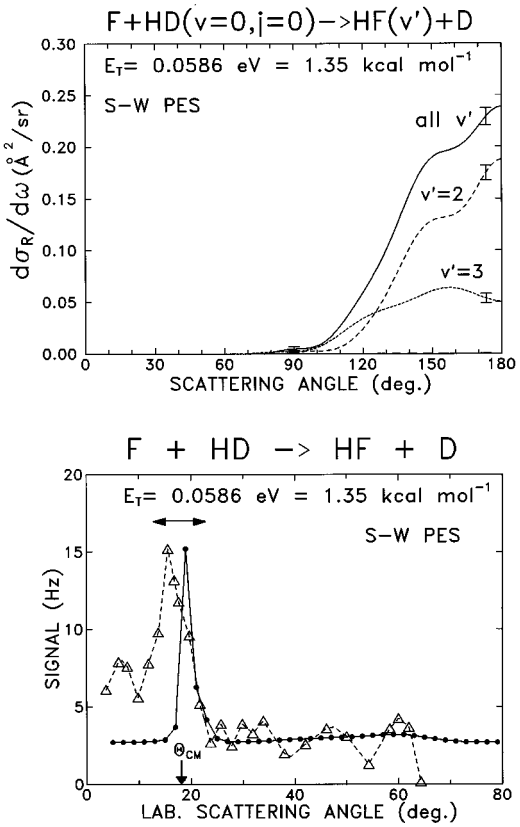

FIG. 6. Top: QCT c.m. differential cross sections for the F+HD $(v=0,j=0)\rightarrow$HF+D reaction at $E_T=58.6$ meV calculated on the SW PES, resolved into the final v' states of HF. Bottom: LAB angular distribution at this collision energy. The triangles and dashed line correspond to the experimental data from Ref. 22 and the solid circles and solid line to the theoretical simulation. The centroid angle $\Theta_{c.m.}$ is indicated with an arrow. The horizontal double side arrow indicates the confinement of the HF $(v'=3)$ product in the LAB system, calculated from the average maximum and minimum LAB Θ angles.

initial rotation in the DCS for the DF channel is almost negligible, similarly to what was found for the integral cross sections. The QCT contribution to the $v'=1$ is very small (see Table I) and, in addition, quite spread in scattering angles, thus making a negligible contribution per solid angle. This seems to be in contrast with the $v'=1$ DCS experimentally deduced, although the only indication of this DCS comes from small signals just above the noise level in the TOF spectra at large LAB scattering angles.

Figure 2 shows the QCT c.m. scattering angle-recoil velocity contour polar map at $E_T=85.9$ meV for the F+HD $\rightarrow$DF+H reaction. This map can be directly compared with the one experimentally deduced (see Fig. 16 of Ref. 22). An inspection of both figures shows that the good agreement found between QCT and experiment is not limited to the c.m. angular distributions, but also extends to the recoil velocities and thus to the product states distribution.

Given the good agreement between QCT results and experimentally deduced DCS in the c.m., an important question to be addressed is the capability of the present QCT calculations to reproduce primary experimental data obtained in the LAB reference system. This is especially interesting since for the rest of the collision energies and for the other isotopic channel, the only available experimental results consist of LAB angular distributions. The simulation of the LAB angular distribution for the DF+H isotopic channel of the reaction at 85.9 meV of collision energy is depicted in Fig. 3 and can be compared with the experimental points. This simulation is made from the QCT vibrorotationally resolved DCS and includes the geometry of the experiment and all the sources of broadening exactly as given in Refs. 21 and 22 (see Sec. II for details on the simulation procedure). There is a remarkable good agreement between simulation and experiment. The contributions of the different vibrational levels to the total AD are also shown in Fig. 3. It can be seen that the scattering into $v'=4$ and $v'=3$ are the main contributions to the experimental peaks at 38° and 50°, respectively. For this collision energy, not only LAB angular distributions but also the TOF spectra of the DF product were simulated for different LAB scattering angles, as shown in Fig. 4, where they are compared with the experimental results. The agreement is excellent with only small discrepancies. It should be stressed that no adjustable parameters are contained in these simulations. This encouraging concordance at the level of primary data in the LAB reference system, at least as good as the one obtained in the c.m. frame, makes possible the extension of the comparison to those results ob-

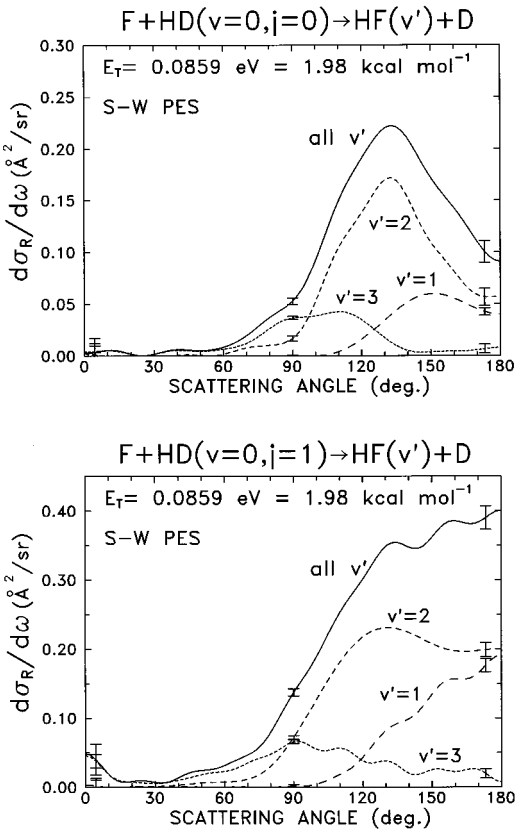

FIG. 7. Center-of-mass solid angle differential cross sections for the F+HD →HF+D reaction, resolved into the final vibrational states, at E_T=85.9 meV for initial $j=0$ (top) and $j=1$ (bottom), calculated by the QCT method on the SW PES. Note the strong influence of HD rotation on the DCS for this isotopic channel.

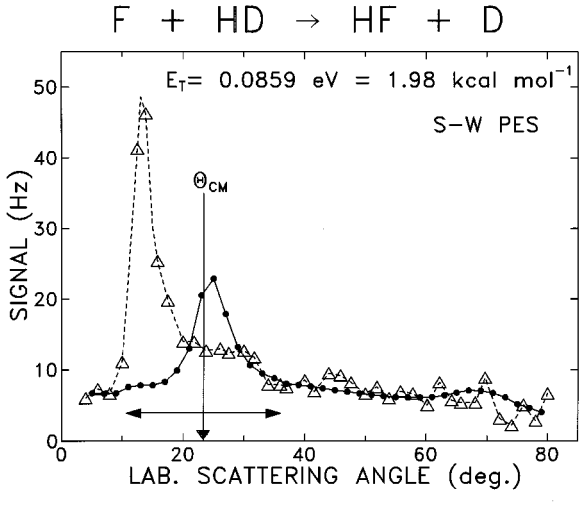

FIG. 8. Experimental (triangles and dashed line) and simulated (solid circles and solid line) LAB angular distributions for the F+HD→HF+D reaction at E_T=85.9 meV. The simulation has been carried out in the same way as for the DF+H channel of the reaction (see Fig. 3). The centroid angle $\Theta_{c.m.}$ is indicated with an arrow. The horizontal double side arrow indicates the confinement of the HF ($v'=3$) product in the LAB system, calculated as in Fig. 6. The simulated data has been scaled to the experimental angular distribution AD using the results from $\Theta=35°$ to 80° (see the text for details).

tained at other collision energies and for both isotopic channels.

Figure 5 shows similar calculations carried out at 58.6 meV (1.35 kcal mol^{-1}) for the DF isotopic channel of the title reaction. The upper panel of this figure portrays the present theoretical c.m. vibrationally resolved DCSs, which are similar to those obtained at E_T=85.9 meV, except for the fact that the scattering is confined to a narrower range of backward angles. The simulation of the LAB angular distribution is shown in the lower panel of this figure, together with the experimental points. The concordance between raw experimental data and the simulation using QCT DCS results is again very satisfactory and shows that present calculations are fully consistent with the existing experimental results. No TOF spectra were reported at this energy, which precludes a more stringent test of the theoretical results.

In the case of the F+HD→HF+D reaction, no TOF spectra were reported at any of the collision energies studied. Given the low signals obtained for the HF product at most of the LAB angles, no faithful c.m. DCS could be deduced.[22] Figure 6 (top) presents the QCT vibrationally resolved DCS at the collision energy of 58.6 meV (1.35 kcal/mol) for the formation of HF+D. The scattering is confined into the backward region and the total DCS is slightly broader than the one obtained for the DF+H channel. Contrary to what happens for the DF channel, the influence of HD rotation for HF formation is decisive, as shown in Table II for the inte-

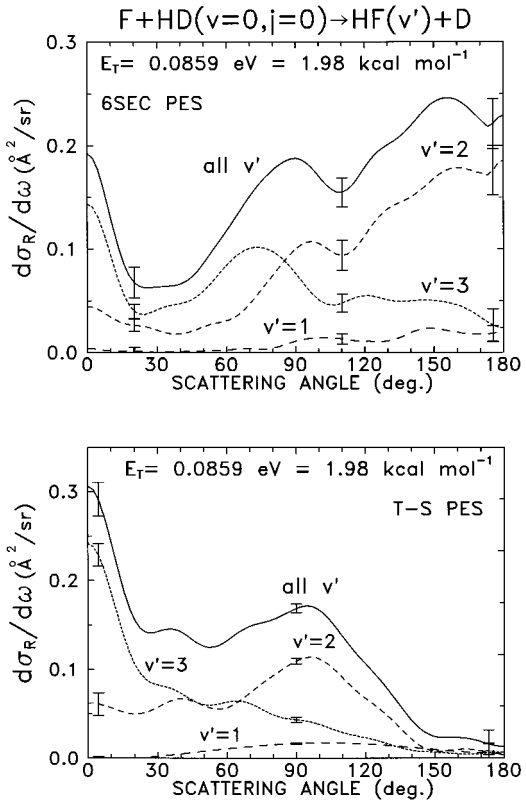

FIG. 9. Center-of-mass solid angle differential cross sections for the F+HD →HF+D reaction resolved into the final vibrational states, at E_T=85.9 meV for initial $j=0$, calculated by the QCT method on the 6SEC PES (top) and on the T-S PES (bottom).

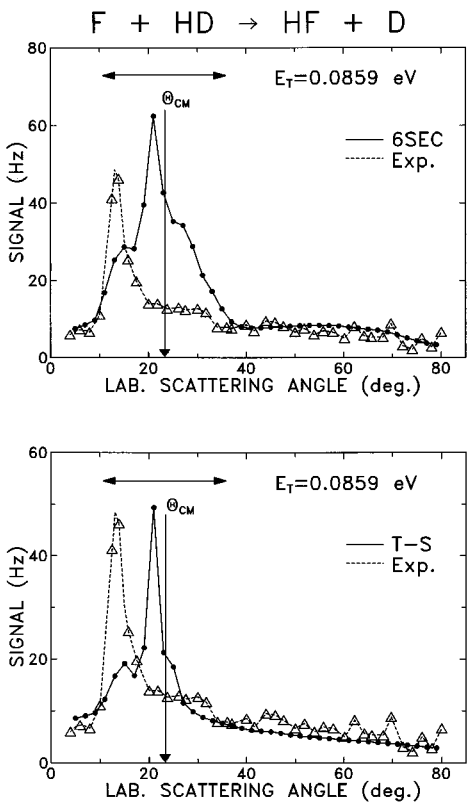

FIG. 10. Experimental (triangles and dashed line) and simulated (solid circles and solid line) LAB angular distributions for the F+HD→HF+D reaction at $E_T=85.9$ meV. The simulation has been carried out as in Fig. 8, using the results calculated on the 6SEC PES (top) and on the T-S PES (bottom). The horizontal double side arrow indicates the confinement of the HF($v'=3$) product in the LAB system. The simulated data has been scaled to the experimental AD using the scaling factor obtained in Fig. 8.

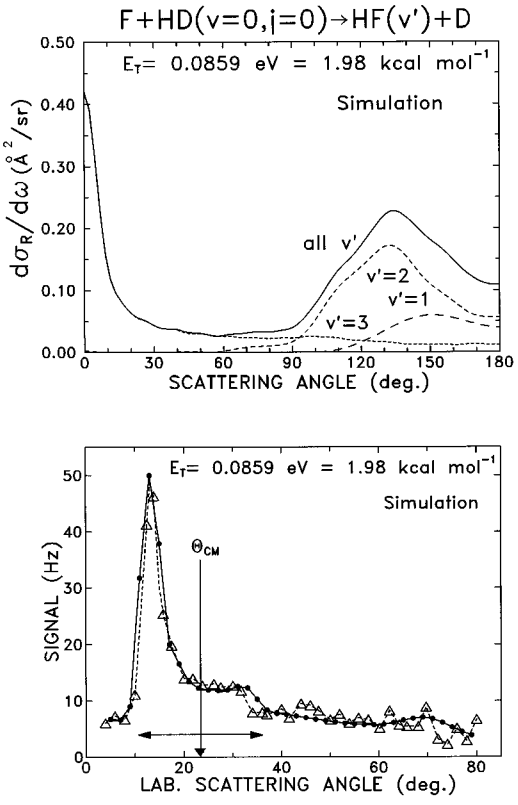

FIG. 11. Top: c.m. vibrationally resolved solid angle DCS obtained by modifying the HF($v'=3$) contribution to the DCS calculated on the SW PES for $j=0$ at the indicated collision energy. Bottom: Comparison of the experimental LAB angular distribution (triangles and dashed line) and the one simulated (solid circles and solid line) by using the c.m. DCS portrayed in the upper panel. The vertical arrow and horizontal double side arrow are as in Fig. 8. It is apparent that a considerable forward peak in $v'=3$ is required to simulate the experiment. The scaling factor is the same as in Figs. 8 and 10.

gral cross sections. However, when going from $j=0$ to $j=1$, there are minor changes in the shape of the c.m. DCS at the collision energy of 58.6 meV (not shown in the figure), except for the emergence of a small contribution of forward scattering (about 10% of the magnitude of the backward peak). The lower panel of Fig. 6 represents the experimental and simulated LAB angular distributions at this energy. The simulation includes the contribution of HD in $j=1$, and the dependence of the reaction cross section in the range of collision energies spanned by the experiment. The location of the average centroid angle, $\Theta_{\text{c.m.}}$, is also indicated in the figure. The main contribution to the LAB angular distribution comes from $v'=3$, highly confined in the LAB system as indicated in the figure by the horizontal double side arrow. In this case, there is a clear disagreement in the location of the peak in the experimental and simulated AD. Whereas the experimental peak appears at LAB angles lower than $\Theta_{\text{c.m.}}$, unequivocally corresponding to forward scattering in the c.m. frame, the simulated one corresponds to c.m. backward scattering, into $v'=3$ and $j'=0$ to $j'=3$.

QCT calculations of the DCS at the collision energy of 85.9 meV (1.98 kcal/mol) for the HF+D channel are shown in Fig. 7 for initial HD rotation numbers $j=0$ and $j=1$. The influence of reagent rotation on the DCS is quite striking. In addition to the above commented effect on the total reactive size, the shapes of the DCS are very different. Backward scattering is much smaller in the absence of rotation and the small forward tail at $j=1$ is not present for $j=0$. Similar effects were also found in the $F+D_2\rightarrow DF+D$ isotopic variant at the collision energy of 144 meV.[48]

Figure 8 shows the corresponding experimental and simulated LAB AD at this collision energy. Also in this case, most of the features in the AD are due to HF ($v'=3$) scattering, which is confined to the range of LAB angles indicated in the figure by the horizontal arrow. The disagreement between experiment and simulation at this energy is even more pronounced than at $E_T=58.6$ meV. Once again, the experimental peak corresponds exclusively to c.m. forward scattering, whereas the simulated one is caused now by HF ($v'=3$) sideways scattered in the c.m. angular range between 60° and 140° (see upper panel of Fig. 7). In view of this discrepancy, the scaling of the simulated data has been made by fitting them to the experimental points from $\Theta=35°$ to 80° [LAB angular range that corresponds to c.m. backward and sideways HF ($v'=1,2$) scattering] using a least squares method and taking into account the experimental base line.

It is clear from what has been commented on above that

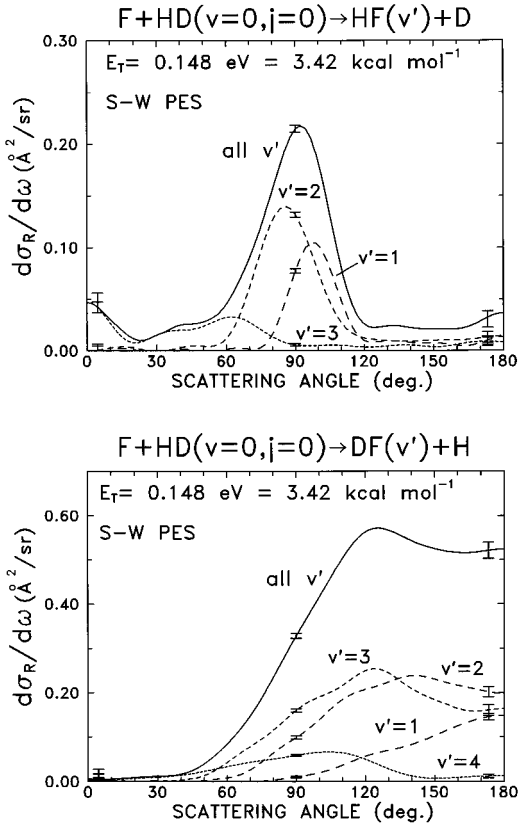

FIG. 12. Center-of-mass solid angle differential cross sections for the HF+D (top) and DF+H (bottom) channels of the title reaction, resolved into the final vibrational states at $E_T=148$ meV for initial $j=0$, calculated by the QCT method on the SW PES. Note the appearance of a clear forward peak and the strong sideways character of the DCS in the HF+D channel.

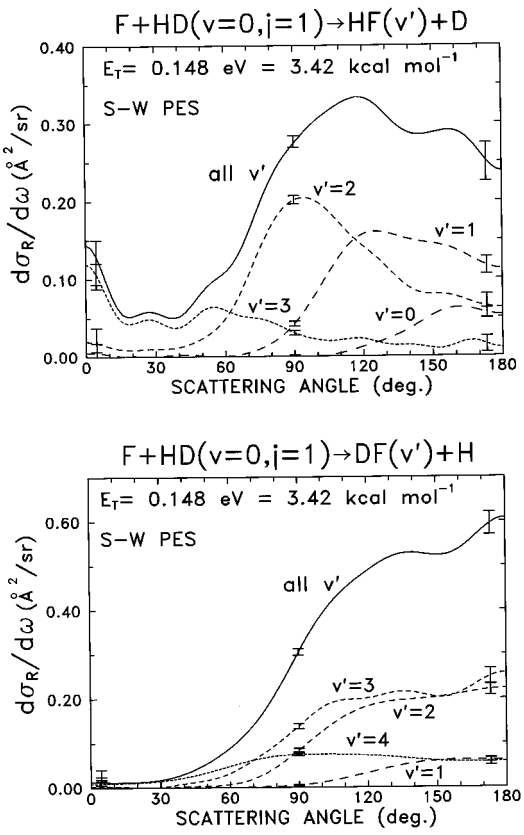

FIG. 13. As in Fig. 12 but for initial $j=1$.

the discrepancies found between the experimental and simulated LAB angular distributions are mainly due to the absence of HF ($v'=3$) forward scattering in the c.m. differential cross sections calculated on the SW PES. One might ask whether there is an intrinsic inability of QCT calculations to reproduce this forward peak. The answer is that the presence of this feature is strictly dependent on the particular PES used in the QCT calculations. In fact, classical calculations[34] for the title reaction on other PES, as the T-S[26] or the 5SEC,[29] give rise to forward scattering at $E_T=85.9$ meV. In the present work, we have repeated the calculations on the T-S PES with sensibly better statistics such that the $v'=3,j'$ state resolved DCS could be determined more precisely and the forward peak could be defined better than in the previous work.[34] In addition, we have carried out calculations on the more recent semiempirical 6SEC PES at the indicated collision energy and for initial $j=0$. Figure 9 shows the vibrationally state resolved c.m. DCS for the F+HD($j=0$)→HF+D reaction calculated on these PES. In both cases, there is a substantial amount of forward scattering in HF ($v'=3$) with smaller contribution from HF ($v'=2$). This fact makes these c.m. DCS good candidates for the simulation of the LAB angular distribution. Figure 10 shows the experimental and simulated AD using the c.m. DCS calculated on the 6SEC and T-S PES. These simulations have been carried out exactly in the same way and using the same scaling factor as the one on the SW PES and, therefore, they are directly comparable.

As expected, both simulations yield contributions in the LAB angular range where the experimental forward scattering is observed. The experimental peak is somewhat better accounted for in the simulation on the 6SEC, however, the overall agreement is indeed very poor. As expected from the c.m. DCS, the simulated AD from the 6SEC is very broad, showing a prominent peak at $\approx 20°$ and two shoulders at $\approx 12°$ and $\approx 25°$, corresponding to HF ($v'=3$) c.m. forward and backward scattering, respectively. The analysis of the peak at $\Theta \approx 20°$ shows that it comes mainly from c.m. HF ($v'=3$) scattering around $\theta \approx 70°$ with some contribution from sideways HF ($v'=2$) scattering ($\theta \approx 90°$). The broad maximum observed in the simulated AD between $\Theta = 40° - 80°$ is the backscattering into HF ($v'=2$).

The agreement between experimental and simulated AD from the T-S PES is even worse. The prominent peak at $\approx 20°$ is also present in the simulation from the T-S PES, but in this case is mainly due to sideways scattering from HF ($v'=2$). The right shoulder at $\approx 25°$ decays rapidly due to the absence of c.m. backward scattering. Although the forward peak in the c.m. v' resolved DCS is larger than in the 6SEC PES, it can be shown that the forward scattering on the T-S PES is rotationally hotter than in any other surface. This causes the c.m. forward scattering to shift in the LAB system towards the centroid angle $\Theta_{\text{c.m.}}$.

Is it possible to produce a c.m. DCS that could account

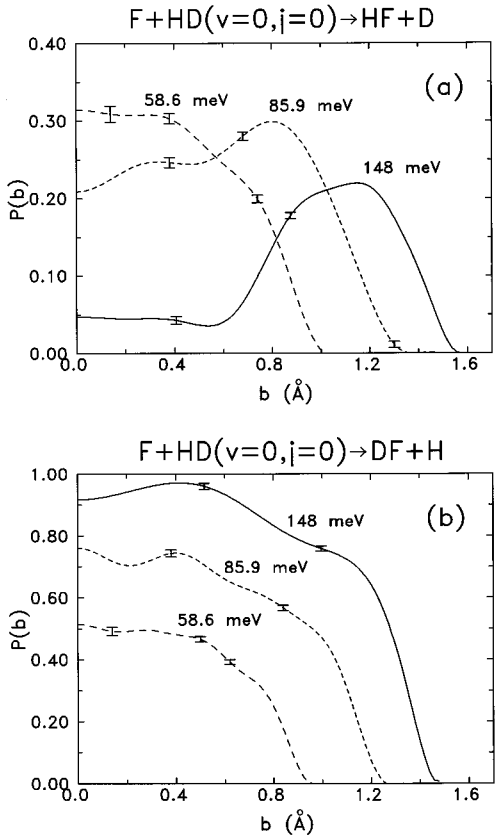

FIG. 14. Reaction probability as a function of impact parameter (opacity function) for the F+HD($v=0,j=0$) reaction at the indicated collision energies. (a) HF+D channel. (b) DF+H channel.

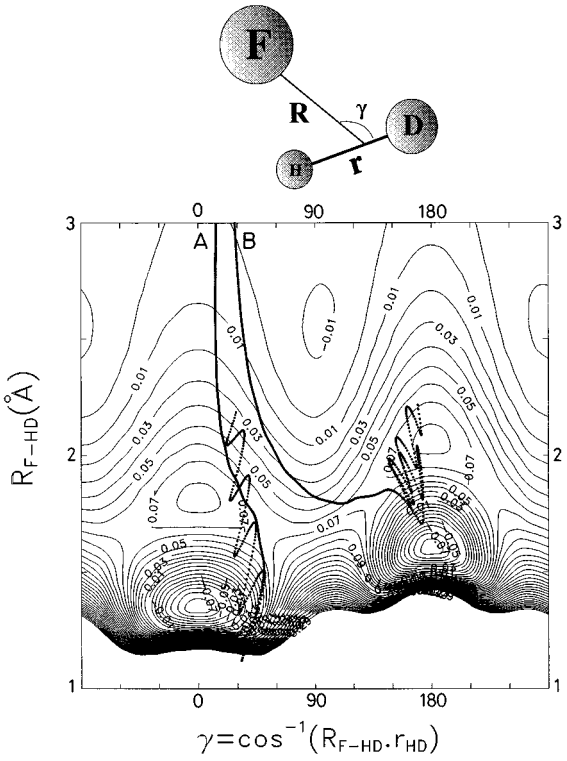

FIG. 15. Contour plot of the SW PES in R,γ coordinates (see the top part of the figure for a definition) at a fixed HD internuclear distance of 0.762 Å (the value at the collinear saddle point). Contour labels are in eV. Two typical trajectories are represented: a nonmigratory trajectory labeled A (the F atom reacts with the end of the molecule which is initially attacked) and a migratory trajectory labeled B (the F atom attacks one of the ends of the molecule reacting with the opposite one). The last one is a typical forward peak trajectory at the collision energy of 148 meV.

for the experimental LAB AD? From the above discussion it is clear that the LAB AD gives little, if any, information on the HF ($v'=1,2$) scattering, especially in the c.m. backward region. It is also clear that a substantial c.m. forward scattering into $v'=3$ is needed to reproduce the experimental LAB AD. Taking into account all the clues obtained from the simulations just presented (Figs. 8 and 10), we have generated c.m. rovibrationally state resolved DCS for the title reaction just by changing the original HF ($v'=3,j'=0,1,2,3$) DCSs, obtained on the SW PES, by DCSs with a forward peak, chosen somewhat arbitrarily to match the experimental peak in the LAB AD. The resulting v' resolved DCS are depicted in the upper panel of Fig. 11. The lower panel of Fig. 11 shows the experimental and simulated LAB AD using the same scaling factor as in Fig. 8. It is clear that in order to reproduce the experimental features, part of the sideways HF ($v'=3$) scattering of Fig. 7(a) has to shift towards low scattering angles, giving rise to a considerable forward peak.

In the case of the F+H_2 reaction, QCT calculations on the SW PES yielded HF ($v'=3$) forward scattering coming from $H_2(j=0)$ when the collision energy was increased from 78.9 to 148 meV. The forward contribution to the DCS increased substantially when going from $j=0$ to $j=1$ at a given collision energy. In any case, the magnitude of the resulting QCT forward scattering for F+n-H_2 (25% in $j=0$ and 75% in $j=1$) was always smaller than the one deduced experimentally.[21,45] It seems therefore interesting to extend this study to higher collision energies even if there is no experimental information available.

Figure 12 portrays the c.m. DCS for the HF+D and DF+H channels of the title reaction at 148 meV and initial HD($j=0$). The evolution of the HF DCS with collision energy is quite remarkable. At this energy, most of the scattering has become sideways with a small forward contribution, whereas the backward scattering has been severely depleted. In contrast, the DF DCS have experienced relatively small changes with respect to the ones at the lower energies. The DCS have become more sideways and therefore broader, especially for $v'=3$ and $v'=4$.

Similarly to what happened at lower collision energies, HD initial rotation affects the two channels in a very different way, as can be seen in Fig. 13. Except for the fact that some backward $v'=3$ and $v'=4$ scattering is recovered when $j=1$, the DCS for the DF+H channel coming from $j=0$ and $j=1$ are quite similar. On the contrary, the v' resolved DCS for the HF+D channel from initial HD ($j=1$) has a greater forward peak and the backward scattering grows dramatically.

IV. DISCUSSION

The results of the previous section demonstrate a very different dynamical behaviour of the two isotopic channels

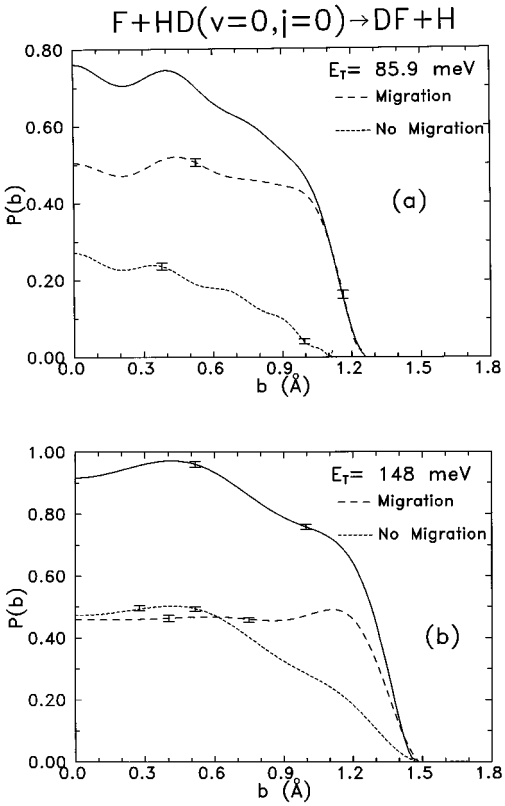

FIG. 16. Opacity functions for the DF+H channel at the indicated collision energies, resolved in the contributions of migrating and nonmigrating trajectories.

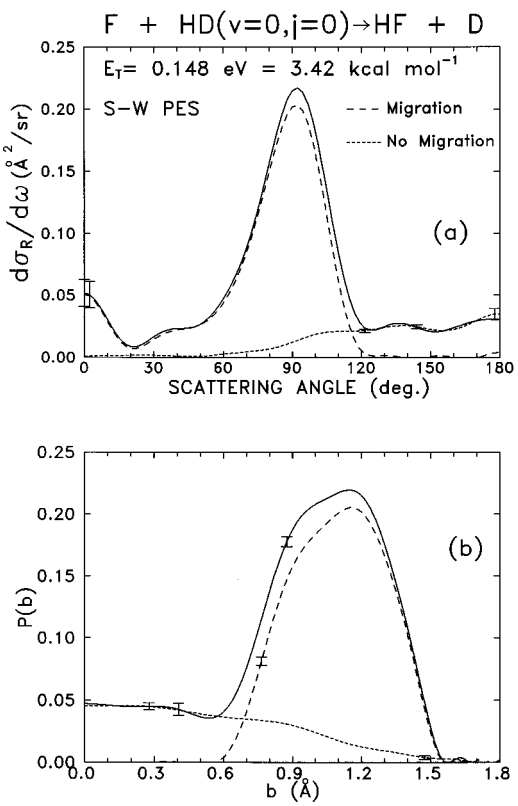

FIG. 17. Center-of-mass solid angle differential cross sections for the F+HD($v=0,j=0$)→HF+D reaction at $E_T=148$ meV, calculated by the QCT method on the SW PES. The dashed lines represent the contribution to the DCS from migrating and nonmigrating trajectories. (b) Opacity function at the same collision energy.

of the F+HD reaction. This is manifest in the integral and differential cross sections and in the influence of the initial rotational angular momentum and translational energy.

In order to gain more insight into the dynamics of this reaction, we have calculated the reaction probability as a function of the impact parameter, i.e., the opacity function $P(b)$, at the three collision energies here studied. Figure 14 shows the results for the two channels and initial $j=0$. The evolution of the opacity functions with the collision energy corresponding to the reaction yielding HF (upper panel) is in strong contrast with that for DF (lower panel). For the DF reaction channel, the shape of the opacity functions changes slightly with the collision energy. It is clear that the increase in $\sigma_R(E_T)$ is caused both by the increase of reaction probability at low b as well as by the participation of larger impact parameters. This is in strong disparity with the opacity functions corresponding to the HF+D channel, where the reaction probability decreases rapidly at low impact parameters as E_T increases. This produces a clear maximum in $P(b)$, that shifts towards higher impact parameters as the collision energy increases. This disappearance of the HF reaction at low b explains why the backward scattering is so drastically depleted as E_T increases in this range of energies and for initial $j=0$.

The next step is then to try to explain all these dynamical results in terms of the features of the potential energy surface and by the analysis of individual trajectories. Among the possible representations of the PES, the contour plot in the $R-\gamma$ coordinate system has been widely used.[36,64,65] Figure 15 depicts this kind of plot for the SW PES and for a HD distance fixed at the value of the collinear saddle point ($r=0.762$ Å). Here R is the distance between the F atom and the center of mass of the HD molecule and γ is the angle between R and the internuclear HD axis r (see insert in Fig. 15). Two caveats should be made about this representation; first, the HD distance is actually not frozen and the potential is changing as the collision proceeds; second, the Jacobi coordinates for the entrance channel, R, r and γ, are of little help in visualizing the exit reactive channel. Nevertheless, at the collision energies studied in this work, the vibration of the HD molecule is fast compared with the F–HD relative motion and, therefore, at sufficiently large distances, the F atom practically sees the HD molecule at rest. Thus, this respresentation provides a good frame for understanding the evolution of the collisions in the entrance channel.

The fact that the center of mass of the HD molecule is closer to the D atom implies that the collisions of fluorine atoms with the H end of the molecule take place at R distances larger than those with the D end. This also causes the cone of acceptance[64] for the reaction with D to be broader than that with H. The PES is quite attractive with two wells in the location of the two atoms and separated by a repulsive wall (that corresponds to sideways attack). On the other hand, the barrier is maximum for collinear approach,

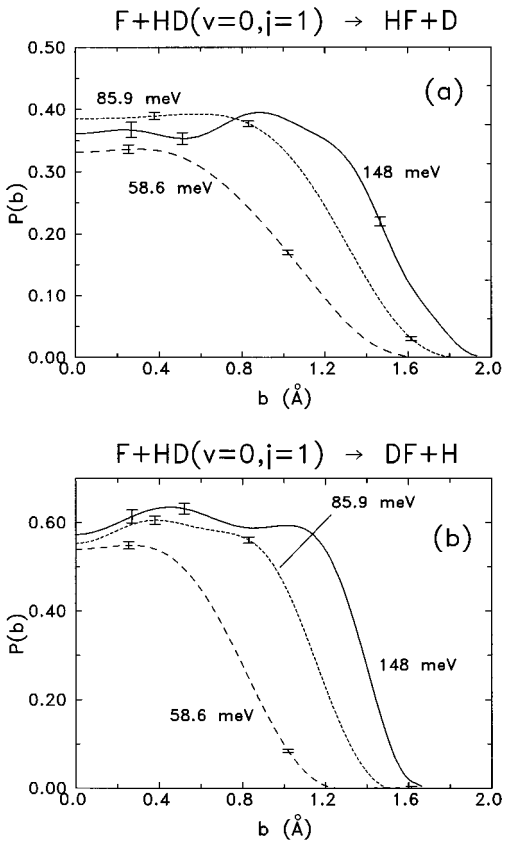

FIG. 18. Opacity functions for the F+HD($v=0,j=1$) reaction at the indicated collision energies. (a) HF+D channel. (b) DF+H channel.

$\gamma=0°$ or 180° ($\approx$85 meV), and minimum for $\gamma\approx45°$. The key feature for the interpretation of the classical results lies on the strong orienting character of this PES. Trajectories attacking either end of the molecule at large distances tend to be oriented towards the opposite side, as it can be seen from the gradient of the potential with γ, $\partial V/\partial\gamma$, that acts as an orientation torque (see the potential contour curves of Fig. 15). Due to the mass asymmetry, this effect is more pronounced for the H side of the molecule.

In a previous work, it was proved that the initial angle of attack, γ_0, plays a decisive role on the dynamics of the $F+H_2$ reaction at zero impact parameter, $b=0$.[36] Trajectories were classified in two groups, "migratory" and "nonmigatory." In the first instance, the fluorine atom reacts with the end of the molecule opposite to the one initially attacked, whereas in the second case reaction takes place with the atom initially attacked. The analysis of individual trajectories in the present work shows that, as long as there is no HD rotation, and since the kinematic orientation due to the orbital angular momentum is small, this classification can be also used for $b\neq0$. Figure 15 depicts two typical trajectories one yielding HF via a migration mechanism, and the other one DF through a nonmigration mechanism.

As a general rule, at low collision energies, trajectories attacking the H side are pulled towards the D side and those attacking the D end tend to be sent to the H side. Since the torque is larger in the H end, this effect is more pronounced for those trajectories in which the atom approaches the molecule at angles between 90° and 180° (see Fig. 15). In fact, it can be shown that at collision energies below 100 meV and for rotationless HD, all the trajectories yielding HF attack initially the D end and therefore are of the migrating type. Both mechanisms, however, participate in the reaction producing DF. At energies below 150 meV, migrating trajectories are predominant, especially for high impact parameters. An increase of the collision energy causes an increase in the energy along R (i.e., the radial energy) and therefore the orienting torque becomes less decisive. Thus contribution from nonmigratory trajectories becomes more important. On the other hand, at a given energy, the migration mechanism predominates for large impact parameters that implies a lower radial energy. This can be seen in Fig. 16 where the opacity functions P(b) for DF formation at two energies are resolved into their migratory ($\gamma_0>90°$) and nonmigratory ($\gamma_0<90°$) contributions.

This also serves to explain why there is a depletion of scattering into the HF channel from low impact parameters (and consequently appearing at high scattering angles) as the collision energy increases (see Fig. 14). Trajectories with low impact parameter that at lower collision energies migrated from the D end to react with the H atom can now give rise to reaction with the D atom via a nonmigrating mechanism. Since the orienting torque is much more important in the H side, this decrease is not compensated by a growth of direct (nonmigrating) trajectories.

The overall behavior of the isotopic branching ratio with the energy is now clearer. Immediately after the threshold, the collision energy favors the DF formation from rotationless HD. As the collision energy increases, both migrating and especially nonmigrating trajectories leading to DF increase. In the HF channel, however, migrating trajectories decrease (selectively for low b) whereas the increase in nonmigrating ones is very slow (at least up to 250 meV).

The analysis of trajectories leading to HF at $E_T=148$ meV illustrates the above comments. Figure 17 shows the differential cross section (upper panel) and the opacity function (lower panel) resolved into the contributions of the two types of trajectories. The sideways and forward scattering, associated with large impact parameters ($b>0.6$ Å), come from migrating trajectories. Interestingly, there is no scattering due to migrating trajectories with $b<0.6$ Å. For this low range of b and $\gamma<90°$ all trajectories produce DF. On the other hand, nonmigrating trajectories that account for the reaction at low impact parameters (and correspondingly backward scattered HF) makes only a small contribution.

Special mention deserves the forward scattering. From the results obtained here, a series of characteristics are found to be common to the majority of the trajectories leading to HF in the forward direction, i.e., to the conspicuous forward peak. The main requisite is a large impact parameter that implies a very low radial energy. In addition, these trajectories only explore the region of the PES around the outer part of the attractive well of the H side, without hitting the inner repulsive wall, corresponding to a typical stripping mechanism. An example of such a trajectory is presented in Fig. 15 (trajectory B). Given the low radial energy at small R char-

acteristic of these forward trajectories, they become extremely sensitive to the details of the PES. At low collision energies, the minimum value of the impact parameter necessary to obtain forward scattering might give a radial energy too small to allow the passage of the barrier. As the collision energy increases, the maximum impact parameter leading to reaction may become large enough to produce forward scattering. For a given b and E_T, the centrifugal barrier is always larger for DF formation (which implies shorter R values). As a consequence, the appearance of forward scattered DF is less likely than that of HF. In fact, for the E_T values of the present work, no DF forward scattering is obtained.

Rotation of the HD molecule diminishes to a great extent the orienting effect of the surface. In fact, rotation is added to the torque exerted by the F atom approaching the HD molecule and can compensate the possible lack of radial energy to overcome the barrier. When HD rotates, the initial angle of attack and, thus, the classification of trajectories into migratory and nonmigratory loses its meaning, since the rotation changes γ several times before the F atom hits either end of the molecule. Figure 18 shows the effect of the rotation on the opacity functions for the two channels of the reaction. In the case of the HF product, the initial rotation of HD has a great effect on the reactivity (compare Figs. 14 and 18). This effect is twofold: On the one hand, the reaction probability at low impact parameters is dramatically enhanced when the rotation increases from HD ($j=0$) to HD ($j=1$), on the other hand, the range of impact parameters for which reaction is possible is significantly enlarged. The observed increase in the DCS forward peak is a consequence of the availability of larger impact parameters. The influence of HD rotation is smaller in the DF+H output channel. In this channel, the range of impact parameters leading to reaction is also enlarged, although not so much as for the HF+D channel, but part of the reactivity at low impact parameters is lost.

Given the enormous influence of rotation in both the integral and differential cross sections, particularly in the HF+D channel, the method chosen for the initial pseudoquantization in the QCT calculations can be of great importance. Throughout this work, the square of the classical rotational angular momentum of the molecule has been equated to $j(j+1)$. The use of the semiclassical quantization[66,67] $(j+\frac{1}{2})^2$, thus adding a "residual" rotation for $j=0$, would make a substantial difference in the outcome. The difference between the two quantization schemes becomes unimportant for $j \geqslant 1$.

The present study demonstrates the key role played by noncollinear collisions on the reactivity of this system and shows the inadequacy of drawing conclusions from the collinear calculations and models that were so popular in the early days of reaction dynamics.

One of the most important conclusions obtained from this and previous works[34] is that whereas the shape of the DCS for the DF channel is similar, very different DCS are obtained for the production of HF on the most currently used PES. Specifically, as shown in Figs. 7 and 9 and Ref. 34, at $E_T=85.9$ meV, all the four surfaces, M5, T-S, 5-SEC (6-SEC) and SW, give rise to very contradictory results. Therefore, even from a pure classical point of view, the scattering into this isotopic channel strongly depends on the topological details of the surface more than in any other isotopic variant of the $F+H_2$ reaction.

In addition, the forward peak appears not necessarily as a pure quantum mechanical effect and its existence and magnitude depend rather on the particular PES, on E_T and on j. The comparison of QCT and QM DCS on the 6SEC PES[35] for the $F+H_2$ reaction suggests, however, that the classical forward peak can be greatly enhanced in quantum mechanical calculations, especially for $j=0$. The high total angular momentum values, J, and low radial energies associated with the forward peak might give rise to interferences and resonances that can explain this enhancement. Thus for F+HD→HF+D reaction, it is likely that accurate QM calculations on the SW PES might yield a DCS more similar to the one of Fig. 11 (i.e., the one needed to reproduce the LAB angular distribution) than the classical result.

On the other hand, based upon past experience with the other isotopic variants, the most important discrepancies between QCT and QM results are expected to be found for the title reaction in the forward scattering coming from $j=0$. Therefore, of all isotopic variants, the HF formation from F+HD is the one where QM effects are expected to be more pronounced.

V. CONCLUSIONS

Quasiclassical trajectory calculations have been carried out for the reaction F+HD on an *ab initio* potential energy surface at the collision energies and initial rotational numbers of the HD molecule necessary to simulate the experiments of Neumark *et al.*[22]

The reactivity into the two channels has been carefully studied and compared with the experimental results of Ref. 22, not only in terms of center of mass (c.m.) differential cross sections (DCS), but also by the simulation of LAB angular distributions and TOF spectra using the data obtained in the present calculations.

For the DF formation, the accordance obtained between the experimentally deduced vibrationally resolved DCS and angle-velocity polar map and those obtained in the present theoretical calculations is excellent. This agreement is even better when the comparison is made between the raw LAB experimental data and their simulations using present QCT results.

In the case of the HF+D reaction channel, there are clear discrepancies between the experimental results available, which consist only of LAB angular distributions, and the theoretical simulations. A close examination of these discrepancies indicates that, in order to reproduce the experimental LAB angular distributions, a large forward peak is needed while the QCT results on the *ab initio* SW PES yield none or little forward scattering at this energy. It is expected that full QM calculations will yield more forward scattering and a better agreement with experiment.

It has been found that the orienting character of the PES plays a major role in the dynamics of this reaction. For rotationless reagents and low collision energies, the surface tends to promote a migratory mechanism; that is, reaction with the opposite end of the molecule that is initially at-

tacked. Rotation of the HD molecule has an enormous influence, especially in the outcome of the HF channel. All this proves that noncollinear collisions are crucial for the reactivity of this system and that a simple analysis in terms of collinear collisions might be misleading.

The discrepancy between the present calculations and the measurements are likely to be due to an insufficiency of classical mechanics, although inaccuracies in the PES or in the experimental data cannot be ruled out completely. All these possibilities deserve a deeper study and should stimulate further work both experimental and theoretical.

ACKNOWLEDGMENTS

The Spanish part of this project has been financed by the DGICYT of Spain (PB92-0219-C03). F.J.A. and V.S.R. acknowledge the German–Spanish Scientific Exchange Program "Acciones Integradas" HA-074, HA-113. The German part of this project was funded by the Deutsche Forschungsgemeinschaft as part of the SFB 216. The *ab initio* calculations were performed on the CRAY-YMP of the Höchstleistungsrechenzentrum Jülich. H.J.W. acknowledges generous support by the German Fonds der Chemischen Industrie, which was partly used to buy the workstations on which part of the present QCT calculations were performed.

[1] G.C. Schatz, J.M. Bowman, and A. Kuppermann, J. Chem. Phys. **58**, 4023 (1973).
[2] G.C. Schatz, J.M. Bowman, and A. Kuppermann, J. Chem. Phys. **63**, 674 (1975).
[3] G.C. Schatz, J.M. Bowman, and A. Kuppermann, J. Chem. Phys. **63**, 685 (1975).
[4] J.T. Muckerman, in *Theoretical Chemistry. Advances and Perspectives*, edited by H. Eyring and D. Henderson (Academic, New York, 1981), Vol. 6A, p. 1.
[5] A. Kuppermann and J.A. Kaye, J. Phys. Chem. **85**, 1969 (1981).
[6] A. Kuppermann, in *Potential Energy Surfaces and Dynamics Calculations*, edited by D.G. Truhlar (Plenum, New York, 1981).
[7] V.K. Babamov and A. Kuppermann, J. Chem. Phys. **77**, 1891 (1982).
[8] J.N.L. Connor, W. Jakubetz, and J. Manz, Mol. Phys. **29**, 347 (1975); **35**, 1301 (1978), and references therein.
[9] M.J. Redmon and R.E. Wyatt, Chem. Phys. Lett. **63**, 209 (1979).
[10] M. Baer, J. Jellinek, and D.J. Kouri, J. Chem. Phys. **78**, 2962 (1983).
[11] R.B. Walker, N.C. Blais, and D.G. Truhlar, J. Chem. Phys. **80**, 246 (1984).
[12] M.J. Berry, J. Chem. Phys. **59**, 6229 (1973), and references therein.
[13] D.S. Perry and J.C. Polanyi, Chem. Phys. **12**, 419 (1976), and references therein.
[14] T.P. Schafer, P.E. Siska, J.M. Parson, F.P. Tully, Y.C. Wong, and Y.T. Lee, J. Chem. Phys. **53**, 3385 (1970).
[15] R.K. Sparks, C.C. Hayden, K. Shobatake, D.M. Neumark, and Y.T. Lee, in *Horizons in Quantum Chemistry*, edited by K. Fukni and B. Pullman (Reidel, Dordrecht, 1980).
[16] J. Jellinek, M. Baer, and D.J. Kouri, Phys. Rev. Lett. **47**, 1588 (1981).
[17] R.E. Wyatt, J.F. McNutt, and M.J. Redmon, Ber. Bunsenges Phys. Chem. **86**, 437 (1982).
[18] K.T. Lee and J.M. Bowman, J. Phys. Chem. **86**, 2289 (1982).
[19] N. Abusalbi, C.L. Shoemaker, and D.J. Kouri, J. Chem. Phys. **80**, 3210 (1984).
[20] E.F. Hayes and R.B. Walker, J. Phys. Chem. **88**, 3318 (1984).
[21] D.M. Neumark, A.M. Wodtke, G.N. Robinson, C.C. Hayden, and Y.T. Lee, J. Chem. Phys. **82**, 3045 (1985).
[22] D.M. Neumark, A.M. Wodtke, G.N. Robinson, C.C. Hayden, R. Shobatake, R.K. Sparks, T.P. Schafer, and Y.T. Lee, J. Chem. Phys. **82**, 3067 (1985).
[23] For work up to 1980 see J.B. Anderson, Adv. Chem. Phys. **41**, 229 (1980), and references therein.
[24] N.C. Blais and D.G. Truhlar, J. Chem. Phys. **76**, 4490 (1982).
[25] S. Ron, M. Baer, and E. Pollak, J. Chem. Phys. **78**, 4414 (1983).
[26] T. Takayanagi and S. Sato, Chem. Phys. Lett. **144**, 191 (1988).
[27] R. Steckler, D.W. Schwenke, F.B. Brown, and D.G. Truhlar, Chem. Phys. Lett. **121**, 475 (1985).
[28] D.W. Schwenke, R. Steckler, F.B. Brown, and D.G. Truhlar, J. Chem. Phys. **84**, 5706 (1986).
[29] G.C. Lynch, R. Steckler, D.W. Schwenke, A.J.C. Varandas, and D.G. Truhlar, J. Chem. Phys. **94**, 7136 (1991).
[30] S.L. Mielke, G.C. Lynch, D.G. Truhlar, and D.W. Schwenke, Chem. Phys. Lett. **213**, 11 (1993); **217**, 173 E (1994).
[31] J.M. Launay and M. Le Dourneuf, ICPEAC XVII Brisbane, July 1991, p. 549.
[32] J.M. Launay, Theor. Chim. Acta **79**, 183 (1991).
[33] F.J. Aoiz, V.J. Herrero, M.M. Nogueira, and V. Sáez Rábanos, Chem. Phys. Lett. **204**, 359 (1993).
[34] F.J. Aoiz, V.J. Herrero, M.M. Nogueira, and V. Sáez Rábanos, Chem. Phys. Lett. **211**, 72 (1993).
[35] F.J. Aoiz, L. Bañares, V.J. Herrero, and V. Sáez Rábanos, Chem. Phys. Lett. **218**, 422 (1994).
[36] F.J. Aoiz, L. Bañares, V.J. Herrero, and V. Sáez Rábanos, Chem. Phys. **187**, 227 (1994).
[37] E. Wurzberg and P.L. Houston, J. Chem. Phys. **72**, 4811 (1980).
[38] R.F. Heidner III, J.F. Bott, C.E. Gardner, and J.E. Melzer, J. Chem. Phys. **72**, 4815 (1980).
[39] R. Atkinson, D.L. Baulch, R.A. Cox, R.F. Hampson, Jr., S.A. Kerr, and J.Troe, J. Phys. Chem. Ref. Data **18**, 88 (1989).
[40] A. Weaver, R.B. Metz, S.E. Bradforth, and D.M Neumark, J. Chem. Phys. **83**, 5352 (1990).
[41] A. Weaver and D.M. Neumark, Faraday Discuss. Chem. Soc. **91**, 5 (1991).
[42] J.Z.H. Zhang, W.H. Miller, A. Weaver, and D. Neumark, Chem. Phys. Lett. **182**, 283 (1991).
[43] S.E. Bradforth, D.W. Arnold, D.M. Neumark, and D.E. Manolopoulos, J. Chem. Phys. **99**, 6345 (1993).
[44] P.J. Knowles, K. Stark, and H.-J. Werner, Chem. Phys. Lett. **185**, 555 (1991).
[45] F.J. Aoiz, L. Bañares, V.J. Herrero, V. Sáez-Rábanos, K. Stark, and H.-J. Werner, Chem. Phys. Lett. **223**, 215 (1994).
[46] K. Stark and H.-J. Werner, J. Chem. Phys. (to be published).
[47] D.E. Manolopoulos, K. Stark, H.J. Werner, D.W. Arnold, S.E. Bradforth, and D.M. Neumark, Science **262**, 1852 (1993).
[48] F.J. Aoiz, L. Bañares, V.J. Herrero, V. Sáez-Rábanos, K. Stark, and H.-J. Werner, J. Phys. Chem. **98**, 10665 (1994).
[49] M. Faubel, L. Rusin, S. Schlemmer, F. Sondermann, U. Tappe, and J.P. Toennies, J. Chem. Phys. **101**, 2106 (1994).
[50] D.E. Manolopoulos, J. Castillo, K. Stark, and H.J. Werner (to be published).
[51] F.J. Aoiz, V.J. Herrero, and V. Sáez Rábanos, J. Chem. Phys. **94**, 7991 (1991).
[52] F.J. Aoiz, V.J. Herrero, and V. Sáez Rábanos, J. Chem. Phys. **97**, 7423 (1992).
[53] K.P. Huber and G. Herzberg, *Molecular Spectra and Molecular Structure, Part IV, Constants of Diatomic Molecules* (Van Nostrand, New York, 1979).
[54] I. Dabrowski and G. Herzberg, Can. J. Phys. **54**, 525 (1976).
[55] W. Kolos and L. Wolniewicz, J. Mol. Struct. **54**, 303 (1975).
[56] D.G. Truhlar and J.T. Muckerman, in *Atom-Molecule Collision Theory*, edited by R.B. Bernstein (Plenum, New York, 1979).
[57] D.G. Truhlar and N.C. Blais, J. Chem. Phys. **67**, 1532 (1977).
[58] N.C. Blais and D.G. Truhlar, J. Chem. Phys. **88**, 5457 (1988).
[59] F.J. Aoiz, L. Bañares, M.J. D'Mello, V.J. Herrero, V. Sáez Rábanos, L. Schnieder, and R.E. Wyatt, J. Chem. Phys. **101**, 5781 (1994).
[60] T.T. Warnock and R.B. Bernstein, J. Chem. Phys. **49**, 1878 (1968); **51**, 4682 E (1969).
[61] R.P. Pack, J. Chem. Phys. **81**, 1841 (1984).
[62] R.E. Contineti, B.A. Balko, and Y.T. Lee, J. Chem. Phys. **93**, 5719 (1990).
[63] D.M. Neumark (private communication).
[64] J.W. Johnston, H. Kornweitz, I. Schechter, A. Persky, B. Katz, R. Bersohn, and R.D. Levine, J. Chem. Phys. **94**, 2749 (1991).
[65] Ju-B. Song and E.A. Gislason, J. Chem. Phys. **99**, 5117 (1993).
[66] M.S. Child, *Molecular Collision Theory* (Academic, London, 1974).
[67] M.S. Child, *Semiclassical Mechanics with Molecular Applications* (Clarendon, Oxford, 1991).